ELSEVIER

Neurobiology of Aging 29 (2008) 1591–1596

NEUROBIOLOGY OF AGING

www.elsevier.com/locate/neuaging

Brief communication

Anatomic localization of the transentorhinal region of the perirhinal cortex

Kirsten I. Taylor [a,b,*], Alphonse Probst [c,a]

[a] *Memory Clinic, Neuropsychology Center, University Hospital Basel, Schanzenstrasse 55, CH-4031 Basel, Switzerland*
[b] *Centre for Speech, Language and the Brain, Department of Experimental Psychology, University of Cambridge, Downing Street, Cambridge, Cambridgeshire CB2 3EB, United Kingdom*
[c] *Department of Neuropathology, University Hospital Basel, Schönbeinstrasse 40, CH-4003 Basel, Switzerland*

Received 15 December 2006; received in revised form 15 February 2007; accepted 23 March 2007
Available online 2 May 2007

Abstract

Brain imaging measures of entorhinal cortex and hippocampus volumes provide valid and reliable markers of Alzheimer's disease (AD). Since AD neurofibrillary pathology begins more laterally in the transentorhinal region (TR) of the perirhinal cortex, volumetric measures of this structure might provide more sensitive preclinical markers of AD, provided its anatomic location is known. The purpose of this study was therefore to define the anatomic location of the TR with respect to the collateral sulcus. Gallyas-stained coronal temporal lobe sections of consecutively autopsied patients were inspected and included in this study if the staining clearly marked the TR ($n = 64$). The number and depths of the collateral sulci were related to the lengths and placement of the TRs. Two patterns emerged: (1) if two discontinuous collateral sulci were present, the TR straddled the more medial and shallow collateral sulcus (8%); (2) if one collateral sulcus was present (91%), the TR included its medial bank. We provide more detailed descriptions of the lateral and medial TR borders for use in volumetric imaging studies.

Keywords: Alzheimer's disease; Neurofibrillary tangles; Transentorhinal cortex; Perirhinal cortex; Collateral sulcus

1. Introduction

A major focus in aging and dementia research is the preclinical detection of Alzheimer's disease (AD). Deficits in episodic memory and measures of entorhinal cortex and hippocampal volumes, structures essential to normal episodic memory functioning, are currently recognized as reliable markers of incipient AD (Almkvist and Winblad, 1999; Csernansky et al., 2005; Dickerson et al., 2001; Jack et al., 1999; Small et al., 2003). These measures are strongly associated with one of the two neuropathological hallmarks of AD: intracellular neurofibrillary tangles and neuropil threads (Bobinski et al., 1996; Delacourte et al., 1999; Gosche et al., 2002; Nagy et al., 1999b; Tiraboschi et al., 2004).

In spite of the focus on episodic memory functioning and its associated structures, neurofibrillary changes associated with AD start neither in the entorhinal cortex nor the hippocampus, but in the neighbouring "transentorhinal cortex" ((Braak and Braak, 1985); corresponding to Stage I (Braak and Braak, 1991)). This region corresponds to Brodmann's cytoarchitectonic field 35 and Van Hoesen and Pandya's field 35a, i.e. the medial portion of the perirhinal cortex (Garey, 1999; Insausti et al., 1987; Van Hoesen and Pandya, 1975). Neurofibrillary pathology proceeds in an orderly, hierarchical fashion, first compromising neurons in the transentorhinal region (TR), then extending medially into layer II of the entorhinal cortex (Stage II) before proceeding to the hippocampus and temporal neocortex (Stage III) and afterwards to adjoining association (Stages IV–V) and primary sensory areas (Stage VI) (Braak and Braak, 1991, 1997; Gertz et al.,

* Corresponding author at: Centre for Speech, Language and the Brain, University of Cambridge, Downing Street, Cambridge CB2 3EB, United Kingdom. Tel.: +44 1223 766 451; fax: +44 1223 766 452.
E-mail addresses: ktaylor@csl.psychol.cam.ac.uk, ktaylor@uhbs.ch (K.I. Taylor), aprobst@uhbs.ch (A. Probst).

0197-4580/$ – see front matter © 2007 Elsevier Inc. All rights reserved.
doi:10.1016/j.neurobiolaging.2007.03.024

1998). Although the "transentorhinal Stages I–II" may begin years and even decades before the diagnosis of AD (Braak and Braak, 1997) and was first considered clinically silent (Braak and Braak, 1991), prospective neuropathological studies have since shown that several of these older individuals were diagnosed with amnestic Mild Cognitive Impairment and even overt dementia within a year of death (e.g. 21% and 21%, respectively (Riley et al., 2002), and 15% and 27% (Bennett et al., 2005), respectively). Significantly, a study by Nagy and colleagues (Nagy et al., 1999a) showed that the majority of individuals in this initial stage where neuropathology is restricted to the TR and entorhinal cortex neurons indeed evidenced a measurable degree of global medial temporal lobe atrophy.

If neurofibrillary AD pathology starts in the TR of the perirhinal cortex and is associated with global measures of anteromedial temporal atrophy detectable on structural imaging scans, then a volumetric measure of the TR alone may provide an even earlier marker of incipient AD than is currently available. This hypothesis has received little attention, perhaps because consensus on the anatomical localization of the human perirhinal cortex was long lacking (Suzuki and Amaral, 2003; Van Hoesen et al., 2000). This is starting to change with Insausti et al.'s (1998) detailed study, which was the first to map the cytoarchitectonic boundaries of this structure in a large group of human autopsy cases ($n = 49$) and provide anatomic landmarks for use in structural imaging studies. Using these guidelines, Juottonen et al. (1998) found that volumes of the entire perirhinal cortex and temporopolar region were reduced in a group of AD patients compared to demographically matched control participants, albeit not as markedly as entorhinal cortex volumes. It remains an open question whether volumetric measures of only the TR would provide more sensitive indicators of dementia pathology than entorhinal cortex volumes, in particular in amnestic Mild Cognitive Impairment as opposed to AD patients. To answer this question, the anatomic location of the TR must first be determined.

The goal of the present study was to determine the anatomic location of the TR in a series of autopsy patients. The TR is defined by an unusual cytoarchitectonic feature: layers III and V of area 35 merge and sweep obliquely towards the pia mater to invade layer II of the entorhinal cortex (area 28), resulting in an oblique layer of neurons (Van Hoesen et al., 2000). This oblique layer of neurons, if affected by neurofibrillary pathology, can be visualized with Gallyas silver staining. It is therefore possible to use Gallyas silver staining as a cytoarchitectonic marker of this region provided a sufficient number of neurons are affected by neurofibrillary pathology. We inspected coronal slices at the level of the anterior hippocampus stained with the Gallyas technique (Gallyas, 1971) in a consecutive series of autopsy patients for visible TRs ($n = 64$). Based on Insausti et al.'s finding that the borders of the perirhinal cortex depend on the depth of the collateral sulcus (cs) (Insausti et al., 1998), we related the depth of the cs to the position of the TR in each case and summarize the relationships between these two measures. Since neurofibrillary pathology is not known to affect the borders (i.e., lengths) of different cytoarchitectonic fields, nor result in more shallow sulci (instead, sulci widen with atrophy), we presume that the relationships between TR lengths and collateral sulcus depths described in the present study apply also to brains not affected by neurofibrillary pathology.

2. Methods

2.1. Materials

All material considered for inclusion in this study was obtained from patients consecutively autopsied at the Department of Pathology, University Hospital Basel, Switzerland, between 1994 and 1996. The whole brain was immersed in formaldehyde (4%) in phosphate-buffered saline (PBS, pH 7.2) for about 2 weeks and the left temporal lobe was subsequently cut in a coronal plane at the level of the anterior hippocampus and the uncal region of the entorhinal cortex. Deparaffinized 5-μm-thick sections (approximately $4\times$ 5 cm) were stained with hematoxilin and eosin, and the Gallyas silver iodide technique (Gallyas, 1971) for the detection of neurofibrillary tangles and neuropil threads. Cases were included in this study if Gallyas silver staining revealed a sufficient number of affected neurons extending from layer II of the entorhinal cortex medially toward a deeper position in the perirhinal cortex laterally where layers III and V merge ((Van Hoesen et al., 2000); $n = 64$; 36 females and 28 males; mean age $\pm$ S.D. $= 83 \pm 7$ years). This oblique layer of neurofibrillary tangles was considered equivalent to the transentorhinal cortex of Braak and Braak (1985). These cases corresponded to Braak and Braak Stages I–VI (mean = 3.3, S.D. = 1.4). These patients had been characterized as neurologically normal ($n = 13$) or had received neurological (or psychiatric) diagnoses of dementia ($n = 37$), cerebrovascular insults ($n = 12$), Parkinson's disease ($n = 7$), depression ($n = 2$), normal pressure hydrocephalus ($n = 2$), essential tremor ($n = 1$), progressive supranuclear palsy ($n = 1$), schizophrenia ($n = 1$) and Wernicke Korsakoff syndrome ($n = 1$) (some patients received multiple diagnoses). Clinical data were not available for two patients who received neuropathological diagnoses of AD (both patients) and intracerebral haemorrhage (one patient).

2.2. Measurements

To determine the anatomic boundaries of the TR in relation to the cs, we measured the depth of the cs in mm from its fundus to the point where a direct line from the fundus to the midpoint of the sulcus at its outermost edge transected a line drawn tangential to the apices of the neighbouring gyri. In cases with two discontinuous cs's (i.e., a shallow, more medial cs located on the convexity of the parahippocampal gyrus and a deeper, more lateral cs located at the boundary of the

parahippocampal and fusiform gyri), the length of the deeper cs was included in the descriptive statistics of the cs. Since the TR was always located on the medial branch of bifurcated cs's (see Section 3), the length of this branch was measured from its fundus to the midpoint of the sulcus at its outermost edge (see also Insausti et al., 1998). The length of the TR was measured in mm from the point where layer II neurons began their descent to the point where they flattened in layer IV of the perirhinal cortex, and this value was also expressed in percent of cs length. TR locations were classified as being located on (1) only the convexity of the parahippocampal gyrus, (2) both the convexity of the parahippocampal gyrus and the medial bank of the cs, (3) only the medial cs bank, (4) both medial and lateral cs banks, or (5) only the lateral cs bank. The lateral and medial edges of the TR were measured in mm from the cs fundus, where negative values indicated a point lateral to the cs fundus and positive values indicated a point medial to the cs fundus, and these values were also expressed in percent of the cs length (see Fig. 1).

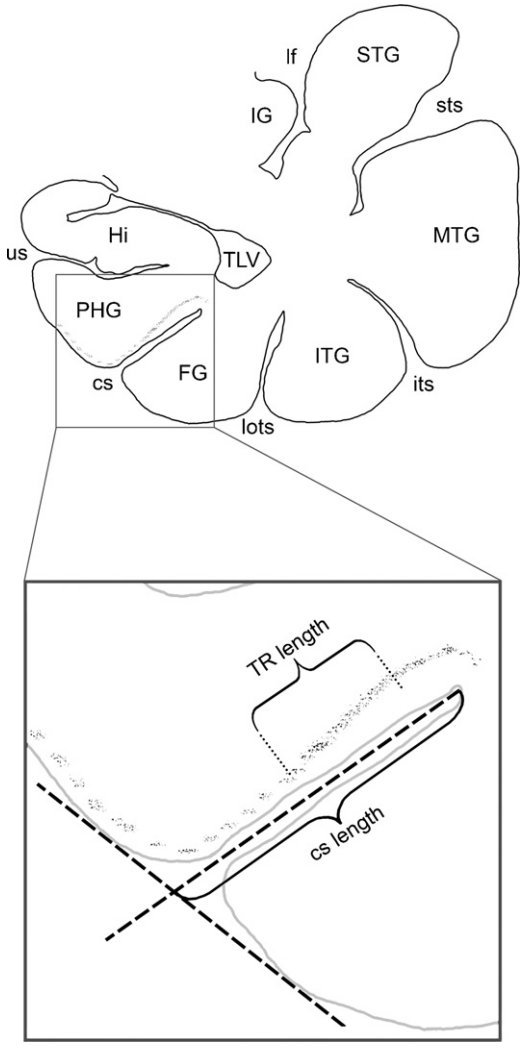

Fig. 1. The upper part of the figure shows the outline of a representative coronal temporal lobe section from the present series with labelled gyri and sulci. The lower part of the figure depicts how the lengths of the collateral sulcus (cs) and transentorhinal region (TR) were measured (see text for details). cs: collateral sulcus; FG: fusiform gyrus; Hi: hippocampus; IG: insular gyrus; ITG: inferior temporal gyrus; its: inferior temporal sulcus; lf: lateral fissure; lots: lateral occipitotemporal sulcus; MTG: middle temporal gyrus; PHG: parahippocampal gyrus; STG: superior temporal gyrus; TLV: temporal horn of lateral ventricle; TR: transentorhinal region; us: uncal sulcus.

3. Results

Descriptive statistics of measurements are presented in Table 1. The mean coronal level of the sections based on the Mai et al. (Insausti et al., 1998) atlas was 14.1 mm, corresponding to a slice including the amygdala, the CA1 and CA2 subfields of the hippocampus, dentate gyrus, subiculum, presubiculum, parasubiculum, uncus, entorhinal cortex and perirhinal cortex (i.e., Talairach and Tournoux, 1988; $y = -14.1$). Two discontinuous cs's were present in five cases (7.8%), and a bifurcated cs was apparent in 10 cases (15.6%). The mean cs depth was 10.1 mm.

The mean length of the TR was 5.3 mm, and TR lengths were significantly positively correlated with cs lengths (Pearson's $r = .368$, $p = .003$). In the ten cases with a bifurcated cs, the TR was always located on its medial branch. The TR was most commonly located on the medial cs bank (42 cases; 65.6%), followed by a location on both the medial and lateral cs banks (14 cases; 21.9%). The TR extended from the medial cs bank onto the convexity of the parahippocampal gyrus in only two cases (3.1%). In six cases (9.4%), the TR was located completely on the convexity of the parahippocampal gyrus. In five of these six cases (8% of all cases), the midpoint of the TR coincided with a sulcus 1 mm in depth which most likely corresponded to discontinuous cs's (R. Insausti, personal communication). Thus, two patterns of TR positions were apparent in the present series: (1) if two discontinuous cs's were present, the TR was located on the more medial and shallow cs (five cases), or (2) if a single cs was present, the TR included its medial bank ($n = 58$). These broad criteria successfully classified 98.4% of cases; in the single misclassified case, the TR was located on the convexity of the parahippocampal gyrus in the absence of a second, discontinuous cs. We describe the lateral and medial TR borders for these two patterns separately. In cases corresponding to the first pattern ($n = 5$), the TR extended on average from 1.9 mm lateral from the medial cs fundus to 2.7 mm medial to this cs. In cases with only one cs (pattern 2), the TR extended on average from 2.8 mm lateral to the cs fundus (or fundus of medial branch in cases with a bifurcated cs) to 8.2 mm along its medial bank (or medial bank of medial branch in cases with a bifurcated cs). The lateral and medial edges of the TR in mm positively correlated with the depth of the cs (lateral edge: Pearson's $r = .746$, $p < .0001$, and medial edge: Pearson's $r = .791$, $p < .0001$): the longer the cs, the more medial were the lateral and medial edges of the TR along the cortical ribbon making up the cs. Thus, the TR borders for cases showing pattern 2 can also be described by the results of linear regression analyses, which take into

Table 1
Descriptive statistics of the coronal level of the sections, collateral sulci (cs) and transentorhinal regions (TR) of the present series of 64 autopsy cases

Measurement	Mean	S.D.	Range	Count	% cases
Coronal Mai atlas level (mm)	14.1	3.2	6.7 to 22.6		
cs characteristics					
Two discontinuous cs's				5	7.8
Bifurcated cs				10	15.6
Length of cs (mm)	10.1	4.4	1.0 to 20.0		
TR characteristics					
Length of TR (mm)	5.3	1.5	2.5 to 9.5		
Length of TR (% of cs)	74.5	80.3	23.1 to 550.0		
TR on convexity of parahippocampal gyrus				6	9.4
TR on convexity of parahippocampal gyrus and medial cs bank				2	3.1
TR on medial cs bank				42	65.6
TR on medial and lateral cs banks				14	21.9
TR on lateral cs bank				0	0
Two cs's: TR on medial cs in parahippocampal gyrus ($n = 5$), measurements with respect medial cs fundus					
Lateral TR border (mm)	−1.9	0.7	−3.0 to −1.0		
Medial TR border (mm)	2.7	0.7	1.5 to 3.0		
One cs: TR on medial bank of cs ($n = 58$), measurements with respect to cs fundus					
Lateral TR border (mm)	2.8	3.9	−4.0 to 11.0		
Medial TR border (mm)	8.2	4.2	2.0 to 16.0		

consideration both the relationship between TR length and cs depth as well as TR position and cs depth: {lateral border of TR in mm from cs fundus = −3.75 + [0.67 × (cs depth in mm)]} (F (1, 56) = 70.27; $p < .0001$) and {medial border of TR in mm from cs fundus = 0.59 + [0.78 × (cs depth in mm)]} (F (1, 56) = 93.62; $p < .0001$). A flowchart for the anatomic location of the TR summarizes these findings (see Fig. 2).

4. Discussion

The present series of Gallyas-stained temporal lobe sections demonstrated an intimate relationship between the cs and TR. The location of the TR was associated with medial aspects of the cs: if two discontinuous cs's were present, the TR always straddled the more medial, shallow cs; if the

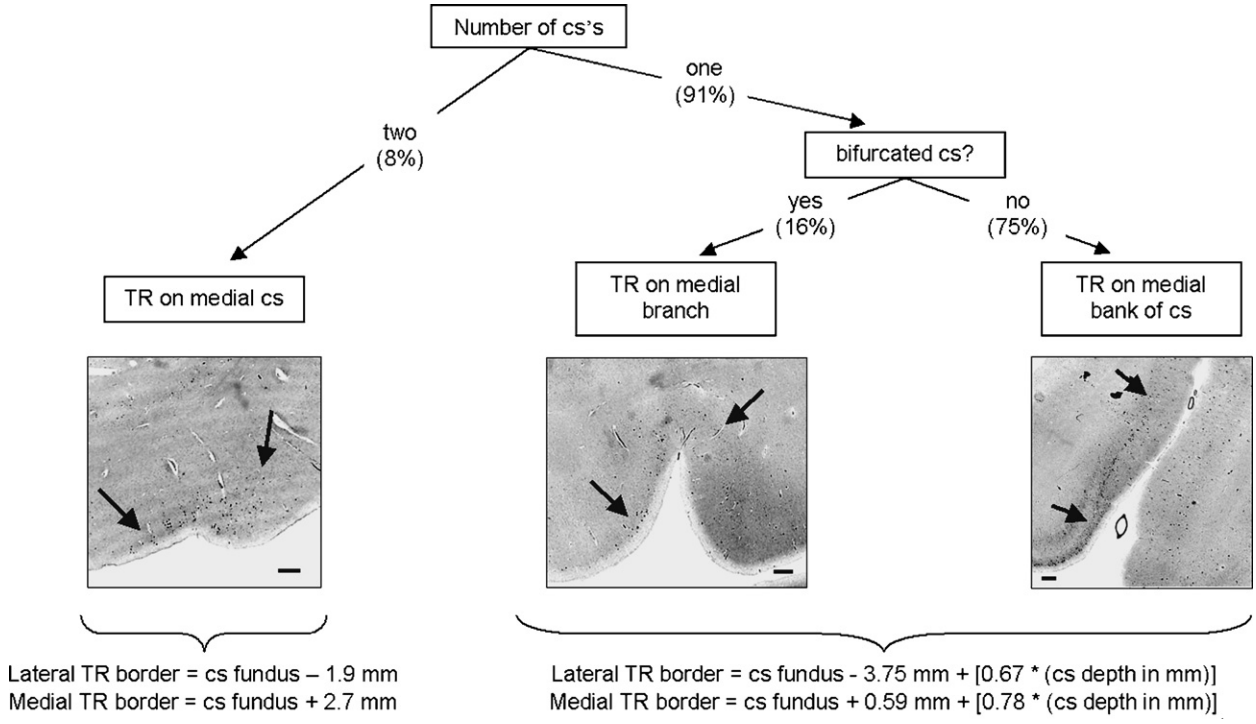

Fig. 2. Flowchart for the localization of the TR (percentages of 64 cases in each instance) with representative coronal, Gallyas-stained temporal lobe sections illustrating the location of the TR (arrows) with respect to the collateral sulci (medial always to the left; bar = 1 mm) and equations for the determination of the lateral and medial borders of the TR in mm with respect to the cs fundus (negative = lateral, positive = medial).

cs was bifurcated (and a discontinuous cs was not present), the TR was always on its medial branch; and perhaps most significantly, the TR strongly favored the medial bank of the cs. While a proper cytoarchitectonic study with healthy and patient brains should be conducted to determine the reproducibility of these results, the patterns we describe are consistent with the findings of Van Hoesen and colleagues who likewise localize area 35 to both the medial and lateral banks of the cs when it is shallow and to the medial branch and fundus of the cs when the cs is of normal depth (Van Hoesen et al., 2000). The present series also demonstrated that deeper cs's were associated both with longer TRs and a more medial position of the TR along the cortical ribbon composing the cs. These findings are consistent with descriptions from Insausti and Amaral (2004), who localized the entorhinal–perirhinal cortex boundary to the medial bank of the cs. More specifically, the cytoarchitectonic study of Insausti and colleagues (Insausti et al., 1998) localized this border at the fundus of shallow cs's (i.e., <1 cm), at the midpoint of the medial cs bank in cs's of regular depth (1–1.5 cm), and at the medial edge of deep cs's (i.e., >1.5 cm). Thus, deeper cs's were likewise associated with a more medial location of the perirhinal–entorhinal cortex boundary in the series of patients studied by Insausti and colleagues. This seminal study described regularities between the location of the perirhinal cortex and the depth of the cs which, significantly, were constant along its entire rostrocaudal extent. Thus, although the relationships we describe between the cs and TR are derived from single temporal lobe slices available from each patient, we suggest that they apply to the entire rostrocaudal extent of the cs. The broad patterns we describe led to the correct anatomic localization of the TR in 98.4% of cases.

The localization of the TR on structural brain images *in vivo* will critically depend on the identification of the cs. While the cs is clearly visible on many coronal slices, the variability in its depth and branching patterns at different rostrocaudal levels make its localization on some individual coronal slices difficult. Pruessner and colleagues (Pruessner et al., 2002) suggest that researchers identify a coronal slice at the level of the posterior hippocampus in which the cs is clearly visible, and follow this sulcus on sagittal images through its rostrocaudal extent (see Pruessner et al., 2002 for details). The present results indicate that the location of the TR will depend on the number and branching pattern of the cs. If two cs's are present, the TR was most commonly positioned on the shallow, more medial cs. This very shallow sulcus most likely corresponds to the end of a discontinuous cs (R. Insausti, personal communication), although some authors classify this sulcus as a rhinal sulcus (Hanke, 1997), and may not be detectable on coronal structural brain images even if its deeper regions can be identified on sagittal slices. If only one cs is present, the boundaries of the TR will depend on the depth of the cs, necessitating its measurement (cf. Insausti et al., 1998; Pruessner et al., 2002). The cs depth can then be entered into the algorithms provided in Fig. 2 to determine the medial and lateral borders of the TR. The anterior and posterior borders of the TR correspond to those of the medial perirhinal cortex (Brodmann's area 35 (Garey, 1999) and Van Hoesen and Pandya's field 35a (Van Hoesen and Pandya, 1975)), and have been described elsewhere (Insausti et al., 1998).

Structural brain imaging has become an important tool in research on aging and AD, and in the diagnosis and differential diagnosis of AD. These studies have established that volumes of the entorhinal cortex and hippocampus are reliably reduced in AD and its purported prodrome, the amnestic Mild Cognitive Impairment syndrome (Almkvist and Winblad, 1999; Small et al., 2003). Since AD neurofibrillary pathology begins in the neighbouring TR, measures of TR cortical thickness or volume based on the patterns of anatomic localization described here may provide researchers with a more sensitive marker of preclinical AD than is currently available.

Disclosure statement

We declare that we have no actual or potential conflicts of interest related to this work.

Acknowledgements

We thank Professor Markus Tolnay for allowing us to access his tissue library, Ms. Sabine Ibsen for processing and staining the tissue samples and Professors H. Braak and R. Insausti for helpful discussions. This study was supported by grants from the Swiss Foundation for Ageing Research (financed by the Loterie Romande), the Freiwillige Akademische Gesellschaft, University of Basel, Switzerland, and the Swiss Alzheimer's Association (KIT).

References

Almkvist, O., Winblad, B., 1999. Early diagnosis of Alzheimer dementia based on clinical and biological factors. Eur. Arch. Psychiatry Clin. Neurosci. 249, 3–9.

Bennett, D.A., Schneider, J.A., Bienias, J.K., Evans, D.A., Wilson, R.S., 2005. Mild cognitive impairment is related to Alzheimer disease pathology and cerebral infarctions. Neurology 64, 834–841.

Bobinski, M., Wegiel, J., Wisniewski, H.M., Tarnawski, M., Bobinski, M., Reisberg, B., De Leon, M.J., Miller, D.C., 1996. Neurofibrillary pathology—correlation with hippocampal formation atrophy in Alzheimer disease. Neurobiol. Aging 17, 909–919.

Braak, H., Braak, E., 1985. On areas of transition between entorhinal allocortex and temporal isocortex in the human brain. Normal morphology and lamina-specific pathology in Alzheimer's disease. Acta Neuropathol. (Berlin) 68, 325–332.

Braak, H., Braak, E., 1991. Neuropathological stageing of Alzhiemer-related changes. Acta Neuropathol. 82, 239–259.

Braak, H., Braak, E., 1997. Frequency of stages of Alzheimer-related lesions in different age categories. Neurobiol. Aging 18, 351–357.

Csernansky, J.G., Wang, L., Swank, J., Miller, J.P., Gado, M., McKeel, D., Miller, M.I., Morris, J.C., 2005. Preclinical detection of Alzheimer's

disease: hippocampal shape and volume predict dementia onset in the elderly. Neuroimage 25, 783–792.

Delacourte, A., David, J.P., Sergeant, N., Buée, L., Wattez, A., Vermersch, P., Ghozali, F., Fallet-Bianco, C., Pasquier, F., Lebert, F., Petit, H., Di Menza, C., 1999. The biochemical pathway of neurofibrillary degeneration in aging and Alzheimer's disease. Neurology 52, 1158–1165.

Dickerson, B.C.G., Goncharova, I., Sullivan, M.P., Forchetti, C., Wilson, R.S., Bennett, D.A., Beckett, L.A., deToledo-Morrell, L., 2001. MRI-derived entorhinal and hippocampal atrophy in incipient and very mild Alzheimer's disease. Neurobiol. Aging 22, 747–754.

Gallyas, F., 1971. Silver staining of Alzheimer's neurofibrillary changes by means of physical development. Acta Morphol. Acad. Sci. Hungaricae 19, 1–8.

Garey, L.J., 1999. Broadmann's 'Localisation in the Cerebral Cortex'. Imperial College Press, London.

Gertz, H.-J., Xuereb, J., Huppert, F., Brayne, C., McGee, M.A., Paykel, E., Harrington, C., Mukaetova-Ladinska, E., Arendt, T., Wischik, C.M., 1998. Examination of the validity of the hierarchical model of neuropathological staging in normal aging and Alzheimer's disease. Acta Neuropathol. 95, 154–158.

Gosche, K.M., Mortimer, J.A., Smith, C.D., Markesbery, W.R., Snowdon, D.A., 2002. Hippocampal volume as an index of Alzheimer neuropathology. Neurology 58, 1476–1482.

Hanke, J., 1997. Sulcal pattern of the anterior parahippocampal gyrus in the human adult. Ann. Anat. 179, 335–339.

Insausti, R., Amaral, D.G., 2004. Hippocampal formation. In: Paxinos, G., Mai, J.K., Paxinos, G., Mai, JKs. (Eds.), The Human Nervous System. Academic Press, San Diego, pp. 871–914.

Insausti, R., Amaral, D.G., Cowan, W.M., 1987. The entorhinal cortex of the monkey. II. Cortical afferents. J. Comp. Neurol. 264, 356–395.

Insausti, R., Juottonen, K., Soininen, H., Insausti, A.M., Partanen, K., Vainio, P., Laakso, M.P., Pitkänen, A., 1998. MR volumetric analysis of the human entorhinal, perirhinal, and temporopolar cortices. Am. J. Neuroradiol. 19, 659–671.

Jack, C.R., Petersen, R.C., Xu, Y.C., O'Brien, P.C., Smith, G.E., Ivnik, R.J., Boeve, B.F., Waring, S.C., Tangalos, E.G., Kokmen, E., 1999. Prediction of AD with MRI-based hippocampal volume in mild cognitive impairment. Neurology 52, 1397–1403.

Juottonen, K., Laakso, M.P., Insausti, R., Lehtovirta, M., Pitkänen, A., Partanen, K., Soininen, H., 1998. Volumes of entorhinal and perhirhinal cortices in Alzheimer's disease. Neurobiol. Aging 19, 15–22.

Nagy, Z., Hindley, N.J., Braak, H., Braak, E., Yilmazer-Hanke, D.M., Schultz, C., Barnetson, L., Jobst, K.A., Smith, A.D., 1999a. Relationship between clinical and radiological diagnostic criteria for Alzheimer's disease and the extent of neuropathology as reflected by 'Stages': a prospective study. Dementia Geriatric Cogn. Dis. 10, 109–114.

Nagy, Z., Hindley, N.J., Braak, H., Braak, E., Yilmazer-Hanke, D.M., Schultz, C., Barnetson, L., King, E.M.-F., Jobst, K.A., Smith, A.D., 1999b. The progression of Alzheimer's disease from limbic regions to the neocortex: clinical, radiological and pathological relationships. Dementia Geriatric Cogn. Dis. 10, 115–120.

Pruessner, J.C., Köhler, S., Crane, J., Pruessner, M., Lord, C., Byrne, A., Kabani, N., Collins, D.L., Evans, A.C., 2002. Volumetry of the temporopolar, perirhinal, entorhinal and parahippocampal cortex from high-resolution MRI images: considering the variability of the collateral sulcus. Cerebral Cortex 12, 1342–1353.

Riley, K.P., Snowdon, D.A., Markesberry, W.R., 2002. Alzheimer's neurofibrillary pathology and the spectrum of cognitive function: findings from the Nun Study. Ann. Neurol. 51, 567–577.

Small, B.J., Mobly, J.L., Laukka, E.J., Jones, S., Backman, L., 2003. Cognitive deficits in preclinical Alzheimer's disease. Acta Neurol. Scand. Suppl 179, 29–33.

Suzuki, W.A., Amaral, D.G., 2003. Where are the perirhinal and parahippocampal cortices? A historical overview of the nomenclature and boundaries applied to the primate medial temporal lobe. Neuroscience 120, 893–906.

Talairach, J., Tournoux, P., 1988. Coplanar Stereotactic Atlas of the Human Brain. George Thieme Verlag, Stuttgart.

Tiraboschi, P., Hansen, L.A., Thal, L.J., Corey-Bloom, J., 2004. The importance of neuritic plaques and tangles to the development and evolution of AD. Neurology, 62.

Van Hoesen, G.W., Augustinack, J.C., Dierking, J., Redman, S.J., Thangavel, R., 2000. The parahippocampal gyrus in Alzheimer's disease: clinical and preclinical neuroanatomical correlates. Ann. N Y Acad. Sci. 911, 254–274.

Van Hoesen, G.W., Pandya, D.N., 1975. Some connections of the entorhinal (area 28) and perirhinal (area 35) cortices of the rhesus monkey. I. Temporal lobe afferents. Brain Res., 95.